

## NEUTRON-RICH HYDROMAGNETIC OUTFLOWS IN GAMMA-RAY BURST SOURCES

NEKTARIOS VLAHAKIS, FANG PENG, AND ARIEH KÖNIGL

Dept. of Astronomy & Astrophysics and Enrico Fermi Inst., Univ. of Chicago, 5640 S. Ellis Ave., Chicago, IL 60637  
vlahakis@jets.uchicago.edu, fpeng@oddjob.uchicago.edu, arieh@jets.uchicago.edu

Submitted to ApJL on June 2, 2003

### ABSTRACT

We demonstrate that “hot” MHD outflows from neutron-rich black-hole debris disks can significantly alleviate the baryon-loading problem in gamma-ray burst (GRB) sources. We argue that the neutron-to-proton ratio in disk-fed outflows might be as high as  $\sim 30$  and show, with the help of an exact semianalytic relativistic-MHD solution, that the neutrons can decouple at a Lorentz factor  $\gamma_d \sim 15$  even as the protons continue to accelerate to  $\gamma_\infty \sim 200$  and end up acquiring  $\sim 30\%$  of the injected energy. We clarify the crucial role that the magnetic field plays in this process and prove that purely hydrodynamic outflows must have  $\gamma_d \gtrsim$  a few  $\times 10^2$ . The motion of the decoupled neutrons is not collinear with that of the decoupled protons, so, in contrast to previous suggestions based on purely hydrodynamic models, the two particle groups do not collide after decoupling. If the decoupled neutrons move at an angle  $\gtrsim 1/\gamma_d \approx 3.8^\circ (15/\gamma_d)$  to the line of sight to the GRB source, most of their emission after they decay into protons will remain unobservable.

*Subject headings:* accretion disks — gamma rays: bursts — MHD — nucleosynthesis — relativity

### 1. INTRODUCTION

Gamma-ray burst (GRBs) are inferred to arise in relativistic outflows of terminal Lorentz factor  $\gamma_\infty \gtrsim 10^2$  (e.g., Lithwick & Sari 2001). In the case of long-duration ( $\Delta t \gtrsim 2$  s) bursts, there is growing evidence that the outflows are highly collimated and involve a kinetic energy  $E_k \sim 10^{51}$  ergs (e.g., Panaitescu & Kumar 2002). The outflows likely originate in a newly formed neutron star (NS) or stellar-mass black hole (BH) and are powered either by the NS or BH spin or by the gravitational potential energy of a remnant accretion disk. The jets can be driven either thermally or magnetically. Magnetic fields offer a natural means of tapping the rotational energy of the source and of guiding, accelerating, and collimating the flow. In a recent series of papers, Vlahakis & Königl [2001, 2003a (VK03a), 2003b (VK03b)] summarized the evidence in favor of magnetic driving as well as previous work on this topic, and presented exact semianalytic solutions of the “hot” relativistic MHD equations demonstrating that Poynting flux-dominated jets can transform  $\gtrsim 50\%$  of their magnetic energy into kinetic energy of  $\gamma_\infty \sim 10^2 - 10^3$  baryons.

The baryonic mass involved in long-duration GRB outflows is estimated to be  $M_p = E_k/\gamma_\infty c^2 \approx 3 \times 10^{-6} (E_k/10^{51} \text{ ergs})(\gamma_\infty/200)^{-1} M_\odot$ . This estimate poses an apparent difficulty for realistic source models. For example, a BH debris disk would need to be a factor  $\sim 10^4$  more massive even if 10% of its gravitational potential energy could be converted into outflow kinetic energy. A question thus arises as to how the baryon loading of the jets remains so low even as the energy deposition in the flow is highly efficient. A promising proposal to alleviate this problem was made by Fuller, Pruet, & Abazajian (2000), who suggested that, if the source of the outflow is neutron-rich, then the neutrons (which are only very weakly affected by the electromagnetic field and are accelerated primarily by collisional drag with ions) could in principle decouple from the flow before the protons attain their terminal Lorentz factor. If the mass source for the flow is a NS then it will clearly be neutron-rich, and this is evidently the case also for outflows fed by a BH debris disk (see § 2). However, it turns out that the decoupling Lorentz factor  $\gamma_d$  in a thermally driven, purely

hydrodynamic (HD) outflow is of the order of the inferred value of  $\gamma_\infty$  (e.g., Derishev, Kocharovskiy, & Kocharovskiy 1999; Beloborodov 2003b; see § 3), which has so far limited the practical implications of the Fuller et al. (2000) proposal. In this Letter we demonstrate that a *hydromagnetic* neutron-rich outflow can go a long way toward addressing the baryon “contamination” problem. In § 2 we consider the composition of GRB disks and construct an illustrative disk model in the context of the supranova scenario for GRBs. A semianalytic MHD solution representing an initially neutron-rich outflow that undergoes decoupling at  $\gamma_d \ll \gamma_\infty$  is presented in § 3. We summarize and discuss the implications of our results in § 4.

### 2. SOURCE COMPOSITION

Pruet, Woosley, & Hoffman (2003) reviewed the various models that attribute GRB outflows to disks around newly formed stellar-mass BHs. They considered disk accretion rates  $\dot{m}_{\text{disk}} \equiv [\dot{M}_{\text{disk}}/(M_\odot \text{ s}^{-1})] = 0.01 - 1$  and viscosity parameters  $\alpha = 0.01 - 0.1$ , and calculated typical midplane electron fractions  $Y_e = \sum_j (Z_j X_j / A_j)$  (where  $Z_j$ ,  $X_j$ , and  $A_j$  are the proton number, mass fraction, and atomic mass number, respectively) near the event horizon of a  $3 M_\odot$  BH in the range  $0.045 - 0.527$  (with  $Y_e$  decreasing with decreasing  $\alpha$  for a given  $\dot{m}_{\text{disk}}$  and increasing with decreasing  $\dot{m}_{\text{disk}}$  for a given  $\alpha$ ). It was argued that material reaching the base of the outflow at the top of the disk would remain neutron-rich if the midplane value of  $Y_e$  were low. Similar results were presented by Beloborodov (2003b).

As a complement to this calculation, we now consider debris disks of the type likely to arise in the supranova scenario for GRBs (Vietri & Stella 1998). In this picture, a supernova explosion leads to the formation of a rapidly rotating, supramassive NS (SMNS), which, after losing rotational support through a combination of electromagnetic and gravitational radiation on a timescale of weeks to years, eventually collapses to a black hole (in the process triggering the GRB). In the original proposal, the debris disk was envisioned to represent the outer layers of an SMNS that were left behind when its central regions collapsed. How-

ever, Shibata, Baumgarte, & Shapiro (2000) argued, on the basis of general-relativistic, 3D hydrodynamic simulations of uniformly rotating stars with a comparatively stiff equation of state (EOS), that the collapse likely involves the entire SMNS. An alternative possibility of forming a disk in stars with a stiff EOS is for matter to be shed centrifugally in the equatorial plane as the SMNS evolves (through the loss of angular momentum) toward the gravitational-instability point. We illustrate this possibility by considering the evolution of such an SMNS along the mass-shedding limit from the maximum-mass point to the maximum-angular-velocity ( $\Omega$ ) point, where it becomes unstable to collapse (see Cook, Shapiro, & Teukolsky 1994). Using the EOS-M equilibrium model results of Cook et al. (1994), we infer that the newly formed BH would have a (gravitational) mass  $M_{\text{BH}} = 2.04 M_{\odot}$  and (assuming that none of the shed mass became unbound) would be surrounded by a debris disk of mass  $M_{\text{disk}} = 0.06 M_{\odot}$ .<sup>1</sup>

Cook et al. (1994) showed that, prior to the formation of the BH, there always exists a region in the equatorial plane outside the SMNS within which particles on circular orbits are unstable to radial perturbations. We thus expect a bona fide accretion disk to form only after the SMNS collapses, and we approximate its initial extent as stretching from the innermost stable circular orbit of the final BH ( $\simeq 4GM_{\text{BH}}/c^2 \approx 12$  km) to the equatorial radius ( $R_e \approx 22$  km) of the Maximum- $M$  configuration (i.e.,  $\Delta\varpi_i \simeq 10$  km, where  $\varpi$  is the cylindrical radius and the subscript  $i$  denotes the base of the flow). Most of the mass would be initially concentrated near the radius of the maximum- $\Omega$  SMNS ( $\simeq 16$  km, henceforth taken to be the typical value of  $\varpi_i$ ), so the disk binding energy can be estimated as  $E_b \approx GM_{\text{BH}}M_{\text{disk}}/\varpi_i \approx 2 \times 10^{52}$  ergs. If we identify a characteristic burst duration of 10 s with the accretion time of the disk, we obtain a fiducial accretion rate of  $\dot{m}_{\text{disk}} = 0.006$ . This rate is below the range considered by Pruet et al. (2003) even as the characteristic midplane density ( $\gtrsim 10^{13}$  g cm<sup>-3</sup>) is much higher than in any of their models. Nevertheless, this disk and the inner regions of most of the Pruet et al. (2003) models share the property that their cooling is dominated by neutrino emission under marginally optically thin conditions. If the outflows from these disks are strongly magnetized, then much of the internal heating could be due to Ohmic dissipation of wound-up magnetic field even as the transport of angular momentum might be dominated by large-scale magnetic stresses (see VK03b). If, however, we represent both of these processes in terms of an  $\alpha$  viscosity, then a rough estimate of the parameter  $\alpha$  for the SMNS-spawned disk can be obtained by equating the accretion time to the viscous angular-momentum transport time in a neutrino-cooled disk model (e.g., Popham, Woosley & Fryer 1999), which yields  $\alpha = 1.2 \times 10^{-3}$ .

We can estimate the density of the innermost mass shell of the maximum- $M$  SMNS that ends up in the disk by setting  $M_{\text{disk}} = [4\pi R_e^4 P_s(\rho_s)/GM][1 - (2GM/R_e c^2)]$  (Lorentz, Ravenhall, & Pethick 1993), which yields  $P_s = 1.5 \times 10^{32}$  dynes cm<sup>-2</sup>. Based on the results of Douchin & Haensel (2001), the corresponding density is  $\rho_s \approx 6 \times 10^{13}$  g cm<sup>-3</sup>, and the shell lies near the bottom of the inner crust and is made up of free neutrons with  $X_n \simeq 0.8$

<sup>1</sup> We neglect any additional mass from the fallback of the original supernova explosion that might surround the BH, as this material would not be as highly magnetized as the SMNS and would therefore be unlikely to partake in the GRB outflow.

and of neutron-rich composite nuclei with  $Z \simeq 40$  and  $Z/A \simeq 1/6$ . The disk mass thus comes mainly from the NS inner crust; the contribution of the outer crust ( $\sim 10^{-4} M_{\odot}$ ) is negligible. After being shed from the NS, the composite nuclei are dissociated and eventually end up releasing their excess neutrons (with the remainder consisting mostly of <sup>4</sup>He). The exact composition of the disk-ejected material is determined by nuclear reactions within the disk (but below the freezeout point, where the nuclear reaction timescale comes to exceed the vertical travel time of the ejected gas) as well as by deuterium and helium production within the flow (e.g., Lemoine 2002; Pruet, Guiles, & Fuller 2002). However, collision with neutrons just prior to decoupling are expected to break apart both  $\alpha$  particles and deuterons (e.g., Pruet et al. 2002; Beloborodov 2003b). In the limit that only free nucleons remain at the time of decoupling, the value of  $Y_e$  for the NS-shed material would be  $\gtrsim 1/30$  and the neutron (n) to proton (p) ratio would be  $(1 - Y_e)/Y_e \lesssim 29$ . Although the n/p ratio at the base of the outflow would be lower than this value, we expect it to be high enough to eventually give rise to n-p drift speeds  $\sim c$  that would lead to decoupling and result in the collisional breakup of the bulk of the remaining composite nuclei.<sup>2</sup> In the illustrative outflow solution presented in § 3 we use a constant pre-decoupling n/p ratio of 30.

### 3. FLOW ACCELERATION AND NEUTRON DECOUPLING

The equations of motion for the neutron component of the outflow are given by

$$(\rho_{0n} U_n^\kappa U_n^\nu)_{,\nu} = \mathcal{F}^\kappa, \quad (1)$$

where  $\rho_{0n}$  is the rest-mass density of neutrons,  $U_n^\kappa = (\gamma_n c, \gamma_n V_n)$  their four-velocity, and

$$\mathcal{F}^\kappa = \frac{\sigma_0 c}{2m_p} \rho_{0p} \rho_{0n} (U^\kappa - U_n^\kappa) \quad (2)$$

the neutron-proton collisional-drag force density.

The rest of the fluid – consisting of protons (with rest-mass density  $\rho_{0p}$ ), radiation (with pressure  $P_R$ ), and  $e^+e^-$  pairs (with pressure  $P_M$ ) – is moving with four-velocity  $U^\kappa = (\gamma c, \gamma V)$ . The equations of motion of the charged fluid component are

$$\left[ \rho_{0p} U^\kappa U^\nu + (P_R + P_M) \left( 4 \frac{U^\kappa U^\nu}{c^2} + \eta^{\kappa\nu} \right) \right]_{,\nu} = \mathcal{F}_{\text{EM}}^\kappa - \mathcal{F}^\kappa, \quad (3)$$

incorporating the p-n drag force density  $-\mathcal{F}^\kappa$  and the electromagnetic force density  $\mathcal{F}_{\text{EM}}^\kappa = [J \cdot E/c, (J^0 E + J \times B)/c]$ . Here  $E$ ,  $B$  is the electromagnetic field and  $J^\nu = (J^0, J)$  the associated four-current (with  $J^0/c$  representing the charge density). As in VK03a, we assume that the photons possess a blackbody distribution (under optically thick conditions) and the pairs a Maxwellian distribution with zero chemical potential. In the large-temperature limit ( $\Theta \equiv k_B T/m_e c^2 \gg 1$ ) the latter corresponds to a 4/3 polytrope,  $P_M \propto \Theta^4 \propto P_R$ ; in this case  $P_M/P_R = 180/\pi^4 \approx 1.85$  is a constant, so the matter and radiation can be treated as a single fluid.

<sup>2</sup> In the “viscous heating and optically thin neutrino cooling” approximation to our debris-disk model, the disk is vertically isothermal and has a temperature  $T_{\text{disk}} = 1.8 \times 10^{10}$  K and a midplane density of  $1.9 \times 10^{13}$  g cm<sup>-3</sup> at  $\varpi_i$ . For the estimated value of  $M_p$  (see § 1) and with  $X_n/X_p = 30$ , the density at the bottom of the disk surface layer that ends up in the flow is  $\rho_{\text{disk}} = 1.2 \times 10^{11}$  g cm<sup>-3</sup> (corresponding to  $\sim 0.1\%$  of  $M_{\text{disk}}$  being ejected). These values of  $T_{\text{disk}}$  and  $\rho_{\text{disk}}$  are comparable to those used in the models of Pruet et al. (2003).

The system (1)–(3), together with Maxwell’s laws and the proton and neutron mass conservation relations can in principle be solved to yield the velocities of the charged ( $U^\kappa$ ) and neutral ( $U_n^\kappa$ ) components as well as the electromagnetic field ( $E, B$ ) and the thermodynamic quantities ( $\rho_{0p}, \rho_{0n}, \Theta$ ). However, a simpler method that is sufficient for our purposes is described below.

During the initial (pre-decoupling) outflow phase, the neutrons and protons are well coupled and their velocities are comparable:  $U_n^\kappa \approx U^\kappa$ . By eliminating the drag force between equations (1) and (3) and setting  $U_n^\kappa \approx U^\kappa$ , we end up with the same system of equations as in the pure proton/lepton case — we only need to replace  $\rho_0$  by  $\rho_{0n} + \rho_{0p} = \rho_{0p}(1 + \rho_{0n}/\rho_{0p})$ . By applying the same  $r$  self-similar model as in VK03a, we can study the neutron-rich outflow and evaluate all the physical quantities, including  $U^\kappa$ . Next, equation (1) with  $U_n^\kappa \approx U^\kappa$  (or eq. [3]) yields the force  $\mathcal{F}^\kappa$ . Finally, equation (2) gives the drift velocity, which can be written (with the help of the continuity equation) as

$$U_n^\kappa - U^\kappa \approx -2m_p U^\nu U_{,\nu}^\kappa / \sigma_0 c \rho_{0p}. \quad (4)$$

So long as the drift velocity is much smaller than the proton velocity, the neutrons remain well coupled to the protons. In the general (nonradial) case there are two possible modes of decoupling, which can be dubbed “along the poloidal field” and “in the transfield direction.” The former happens when the relative velocity between protons and neutrons along the poloidal magnetic field,  $V_{\parallel} - V_{n\parallel}$ , grows to  $\sim V_{\parallel} \approx c$ , and the latter when  $V_{n\perp}$  becomes  $\sim \Delta \omega \cos \vartheta / \gamma \tau_{\text{dyn}}$ , where  $\vartheta$  is the jet opening half-angle,  $\Delta \omega \cos \vartheta$  is its width, and  $\tau_{\text{dyn}} \sim z/\gamma c$  is the dynamical timescale. (The subscripts  $\parallel, \perp$  denote components of a vector along the poloidal magnetic field and in the transfield direction, respectively.)

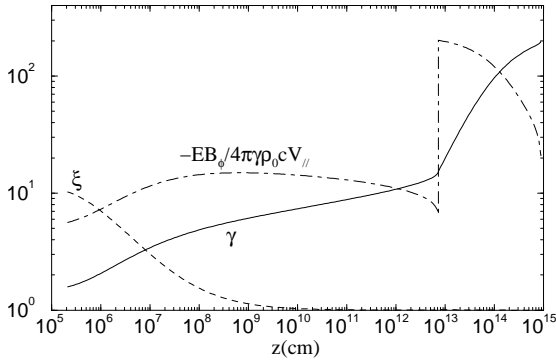


FIG. 1.— Lorentz factor  $\gamma$  (solid), specific enthalpy  $\xi = (\rho_0 c^2 + 4P_R + 4P_M)/\rho_0 c^2$  (dashed), and Poynting-to-mass flux ratio  $-(c/4\pi)EB_\phi/\gamma\rho_0 c^2 V_{\parallel}$  (dot-dashed) as functions of height ( $z$ ) along the innermost fieldline. Here  $\rho_0 = \rho_{0n} + \rho_{0p}$  below the decoupling point and  $\rho_0 = \rho_{0p}$  above it. The baryon mass-normalized quantities are discontinuous at the decoupling transition, where they increase by a factor  $1 + \rho_{0n}/\rho_{0p}$ .

We model the post-decoupling evolution of the charged fluid component using the same  $r$  self-similar model used in the pre-decoupling phase (but replacing  $\rho_0$  by  $\rho_{0p}$ ). Figures 1 and 2 show a solution representing an outflow from a disk with an inner radius  $r_{\text{in}} = 1.2 \times 10^6$  cm and outer radius  $r_{\text{out}} = 2r_{\text{in}}$ . The initial conditions for the innermost fieldline ( $r_1 = r_{\text{in}}, \theta_1 = 80^\circ$ ) are:  $\rho_{0n}/\rho_{0p} = 30, \rho_{0n} + \rho_{0p} = 10^5$  g cm $^{-3}, \Theta = 2.2, B_p = 10^{12}$  G,  $B_\phi = -10^{14}$  G,  $\vartheta = 55^\circ, V_p = 0.6916c$ , and  $V_\phi = 0.35c$ .<sup>3</sup> These conditions correspond to a rough equipartition between comoving magnetic and thermal pressures —

<sup>3</sup> The value of the model parameter  $F$  is 1.05 before decoupling and 0.1

$(B^2 - E^2)/8\pi(P_R + P_M) = 1.0$ , a total outflowing baryon mass  $M_b = 2 \iint \gamma \rho_0 V \cdot dS \Delta t = 9.22 \times 10^{-5} (\Delta t/10\text{s}) M_\odot$ , and total energy  $\mathcal{E}_i = 3.62 \times 10^{51} (\Delta t/10\text{s})$  ergs. The various components of the initial total energy are [electromagnetic, enthalpy (including rest energy), kinetic] =  $[5.615, 15.631, 0.583] \times M_b c^2$ . During the pre-decoupling phase, part of the enthalpy is converted into baryon kinetic energy (resulting in an increase in  $\gamma$ ) and another is converted into electromagnetic energy (resulting in an increase in the Poynting-to-mass flux ratio; see Fig. 1). Above  $z \approx 10^9$  cm the fluid is practically cold ( $P_R + P_M \ll \rho_0 c^2 \Leftrightarrow \xi \approx 1$ ) and the magnetic field is starting to accelerate the matter: in this regime the increasing  $\gamma$  corresponds to a decreasing Poynting-to-matter flux ratio.

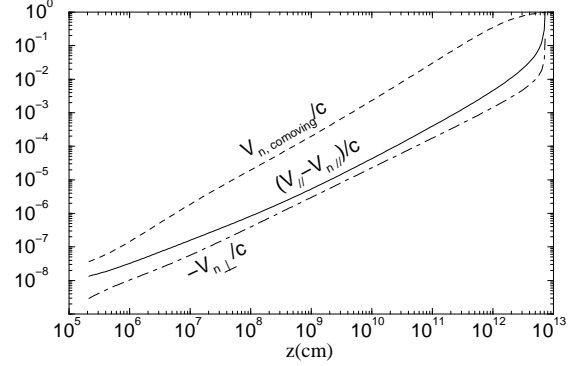


FIG. 2.— Proton–neutron drift velocity along the poloidal magnetic field (solid), in the transfield direction (dot-dashed), and in the comoving proton frame (dashed) for the outflow described in Fig. 1.

Figure 2 shows the various components of the drift velocity. At  $z = z_d \approx 7 \times 10^{12}$  cm,  $V_{\parallel} - V_{n\parallel} \sim c$  and the neutrons decouple from the protons. In this particular solution the “along the flow” decoupling happens first, although at the time of decoupling the neutrons also have a nonnegligible outward-directed transfield velocity component ( $V_{n\perp} \sim 0.1c \ll V_{n\parallel}$ ). The latter component arises from the ongoing magnetic collimation of the jet: by the time the flow reaches  $z_d$ ,  $\vartheta$  is already decreased to  $\sim 7^\circ$ .<sup>4</sup> At the decoupling point  $\gamma = \gamma_d \approx 15.3$ , and the energy of the charged fluid component is  $\mathcal{E}_{c,d} = 1.16 \times 10^{51} (\Delta t/10\text{s})$  ergs = 32%  $\mathcal{E}_i$  [with the remaining 68% residing in the neutron kinetic and rest energies,  $\gamma_d M_b c^2 / (1 + \rho_{0p}/\rho_{0n})$ ]. In units of the proton rest energy  $M_p c^2 = M_b c^2 / (1 + \rho_{0n}/\rho_{0p})$ , the various components of this energy are [electromagnetic, enthalpy (including rest energy), kinetic] =  $[201.79, 1.22, 14.31] \times M_p c^2$ .

Above  $z_d$  we continue the integration of equation (3) with  $\mathcal{F}^\kappa = 0$ . Figure 1 shows that the acceleration in this regime is magnetic: the electromagnetic energy decreases and the Lorentz force accelerates the protons to a terminal Lorentz factor  $\gamma_\infty = 200$ . The final proton kinetic energy is  $E_k = \gamma_\infty M_p c^2 \approx \mathcal{E}_{c,d}$ , indicating that the acceleration efficiency in the post-decoupling region is  $\approx 100\%$ .

The above solution demonstrates that, in contrast to the HD case considered by previous authors, neutron decoupling in an MHD outflow can occur with  $\gamma_d \ll \gamma_\infty$ . To understand why

after decoupling. We use the form of the n-p collisional cross section given in Derishev et al. (1999), with  $\sigma_0 = 3 \times 10^{-26}$  cm $^2$ .

<sup>4</sup> The value of  $\vartheta$  for the proton component changes little after decoupling; to obtain the exact value of the angle between the two particle species at the time of decoupling, the system of equations (1)–(3) must be solved without the approximation  $U_n^\kappa \approx U^\kappa$ .

magnetic acceleration is crucial to this outcome, consider approximating the local scaling of the Lorentz factor with cylindrical radius by  $\gamma \propto \bar{\omega}^{\delta_1}$  and the fieldline (or streamline) shape by  $r \approx z \propto \bar{\omega}^{1+\delta_2}$ , where  $\delta_1, \delta_2$  are positive constants. Under the approximation of exact mass conservation for the proton component,  $\gamma \rho_{0p} \propto \bar{\omega}^{-2}$ . At the decoupling point  $\tau_{\text{coll}} \approx \tau_{\text{dyn}}$ , where  $\tau_{\text{coll}} = m_p / \sigma_0 c \rho_{0p}$ .<sup>5</sup> Using the above scalings, we obtain  $\gamma_d = \gamma_i (\rho_{0p,i} r_i \sigma_0 / m_p \gamma_i)^{\delta_1 / (2\delta_1 + 1 - \delta_2)}$  and  $r_d = r_i (\gamma_d / \gamma_i)^{(1+\delta_2) / \delta_1}$ . In the HD case, the energy equation  $\xi \gamma \propto \Theta \gamma = \text{const}$  and the polytropic relation  $\Theta^4 \propto \rho_{0p}^{4/3}$  always imply a linear increase of  $\gamma$  with  $\bar{\omega}$ . Thus,  $\delta_1 = 1$  in this case, and the minimum value of  $\gamma_d$ ,  $\gamma_{d\text{HDmin}} = \gamma_i (\rho_{0p,i} r_i \sigma_0 / m_p \gamma_i)^{1/3}$ , is attained in a conical flow ( $\delta_2 = 0$ ). For typical values of the source size (at least  $10^6$  cm) and initial proton density<sup>6</sup> (at least a few times  $10^2$  g cm<sup>-3</sup>),  $\gamma_{d\text{HDmin}}$  is a few times  $10^2$ . On the other hand, in MHD flows where a significant part of the enthalpy can be initially transferred into Poynting energy, the pre-decoupling acceleration is slower, corresponding to  $\delta_1 < 1$ . (In the solution presented here,  $\delta_1 \approx 0.13$  and  $\delta_2 \approx 0.15$ .) This makes it possible for  $\gamma_d$  to be  $\ll \gamma_{d\text{HDmin}}$ . The energy deposited in the Poynting flux is subsequently returned to the matter as kinetic energy, enhancing the fraction of the total energy used to accelerate the proton component.

#### 4. SUMMARY AND IMPLICATIONS

We argued that GRB outflows emanating from accreting debris disks around stellar-mass black holes could possess a high ( $\lesssim 30$ ) pre-decoupling neutron-to-proton mass ratio, and we demonstrated semianalytically, by means of a “hot” relativistic-MHD solution, that n-p decoupling can occur at a Lorentz factor ( $\gamma_d \approx 15$  in the presented example) that is significantly lower than the terminal  $\gamma$  of the protons ( $\gamma_\infty = 200$  in our solution). We explained why, in contrast,  $\gamma_d$  cannot be smaller than a few times  $10^2$  if the acceleration is purely hydrodynamic. In the outflow solution that we constructed, the protons, while constituting only  $\sim 3\%$  of the ejected mass, end up with a kinetic energy  $\sim 10^{51}$  ergs that represents  $\sim 1/3$  of the injected energy (with the remainder going to neutron kinetic energy).

This could significantly alleviate the baryon-loading problem in GRB source models. For example, in the illustrative SMNS-shed disk model that we considered, the outflow rate represents  $\sim 0.1\%$  of the mass inflow rate. If a fraction of

this order of the disk mass can be ejected (with  $X_n/X_p$  that becomes  $\sim 30$  just before decoupling) in a “hot” magnetized jet, then it may not be necessary to consider alternative sources of energy or mass for GRB outflows, for which the converse problem (how to avoid having too few baryons) is often encountered (e.g., Levinson & Eichler 2003).

The decoupled neutrons decay into protons at a distance  $r_\beta = \gamma_d c \tau_\beta \approx 4 \times 10^{14} (\gamma_d / 15)$  cm, where  $\tau_\beta \approx 900$  s is the comoving decay time. Nonthermal shock-induced emission from the resulting charged-particle shell may be hampered by the lack of a strong magnetic field unless significant field amplification occurs in the shocks themselves (e.g., Beloborodov 2003a) or if the neutrons propagate within a highly magnetized medium (as might happen in the supranova scenario; Königl & Granot 2002). Internal collisions arising from the same velocity perturbations that are invoked to account for the observed  $\gamma$ -ray emission in the internal-shock scenario would typically occur on a scale  $\ll r_\beta$  and thus (in contrast to the situation in the proton shell) would not give rise to radiative shocks. Emission might, however, be expected from the reverse shock driven into the decaying neutron shell as it starts to decelerate. Most of this shell’s kinetic energy would, however, be radiated from the external shock that is driven into the ambient gas. The bulk of the radiation would be emitted at the distance  $r_{\text{dec,n}}$  where the mass swept up from the ambient medium comes to exceed  $\sim 1/\gamma_d$  of the shell mass. This would occur on a timescale  $\sim r_{\text{dec,n}} / 2\gamma_d^2 c$ , which, for a uniform environment, is a factor  $\sim 10^3 (X_n / 30X_p)^{1/3} (\gamma_\infty / 13\gamma_d)^{7/3}$  larger than the corresponding timescale for the original proton shell. Most of this emission would, however, remain undetectable if the angle between the neutron-shell velocity and the line of sight exceeded  $\sim 1/\gamma_d \approx 3.8^\circ (15/\gamma_d)$ . It is in any case clear that the transverse n-p relative motion at the time of decoupling precludes any subsequent interactions between the two shells (see, e.g., Pruet & Dalal 2002 and Beloborodov 2003a). A detailed consideration of the possible observational signatures of the neutron shell remains an interesting problem for future research.

We thank Andrei Beloborodov, Gregory Cook, Jason Pruet, and Stuart Shapiro for helpful discussions and correspondence. This work was supported in part by NASA grant NAG5-12635.

inferred from  $M_p = E_k / \gamma_\infty c^2$  using  $E_k \sim 10^{51}$  ergs and  $\gamma_\infty = \text{a few} \times 10^2$ .

<sup>5</sup> A more exact condition for the decoupling comes from eq. (4), which implies  $V_{\parallel} - V_{\text{nl}} \sim c \Leftrightarrow 2(m_p / \sigma_0 \rho_{0p}) d\gamma / dz \sim 1$ , or  $\tau_{\text{dyn}} \sim (2d \ln \gamma / d \ln z) \tau_{\text{coll}}$ .

<sup>6</sup> As a rough estimate,  $\rho_{0p,i} \sim M_p / 4\pi r_i^2 c \Delta t$ , with the ejected proton mass

#### REFERENCES

- Beloborodov, A. M. 2003a, ApJ, 585, L19  
 Beloborodov, A. M. 2003b, ApJ, 588, 931  
 Cook, G. B., Shapiro, S. L., & Teukolsky, S. A. 1994, ApJ, 424, 823  
 Derishev, E. V., Kocharovskiy, V. V., & Kocharovskiy, V. I. 1999, ApJ, 521, 640  
 Douchin, F., & Haensel, P. 2001, A&A, 380, 151  
 Fuller, G. M., Pruet, J., & Abazajian, K. 2000, Phys. Rev. Lett., 85, 2673  
 Königl, A., & Granot, J. 2002, ApJ, 574, 134  
 Lemoine, M. 2002, A&A, 390, L31  
 Levinson, A., & Eichler, D. 2003, ApJ, submitted (astro-ph/0302569)  
 Lithwick, Y., & Sari, R. 2001, ApJ, 555, 540  
 Lorentz, C. P., Ravenhall, D. G., & Pethick, C. J. 1993, Phys. Rev. Lett., 70, 379  
 Panaitescu, A., & Kumar, P. 2002, ApJ, 571, 779  
 Popham, R., Woosley, S. E., & Fryer, C. 1999, ApJ, 518, 356  
 Pruet, J., & Dalal, N. 2002, ApJ, 573, 770  
 Pruet, J., Guiles, S., & Fuller, G. M. 2002, ApJ, 580, 368  
 Pruet, J., Woosley, S. E., & Hoffman, R. D. 2003, ApJ, 586, 1254  
 Shibata, M., Baumgarte, T. W., & Shapiro, S. L. 2000, Phys. Rev. D, 61, 4012  
 Vietri, M., & Stella, L. 1998, ApJ, 507, L45  
 Vlahakis, N., & Königl, A. 2001, ApJ, 563, L129  
 Vlahakis, N., & Königl, A. 2003a, ApJ, submitted (VK03a)  
 Vlahakis, N., & Königl, A. 2003b, ApJ, submitted (VK03b)